Modelling heat transfer through a novel design of rotary kiln

Modelling heat transfer through a novel design of rotary kiln

J.K. Martin*, R.J. Matela† and R.G. Sherwen‡

*Department of Environmental and Mechanical Engineering, Milton Keynes, Bucks MK7 6AA, UK
E-mail: j.k.martin@open.ac.uk

†Department of Design, The Open University, Milton Keynes, Bucks MK7 6AA, UK

‡Sherwen Engineering Co Ltd., Dartford, Kent DA2 8EB, UK
E-mail: Ronald.Sherwen@btinternet.com

Abstract: A novel form of rotary kiln has been developed which confers advantages over conventional designs. Details are given of the main features of the kiln, along with an approach used to study its heat transfer characteristics when hot processing waste products into a lightweight synthetic aggregate for recycling in building materials. Computer aided finite element modelling was used to predict temperature profiles and heat fluxes involving non-linear properties of the exterior insulation materials and internal radiation effects. Observations are given comparing predicted temperatures for two different cross sectional shapes and with those measured in practice on a prototype novel kiln. Observations are also given on the methods of approach to the modelling.

Keywords: rotary kiln, waste processing, finite element modelling, thermodynamic performance.

Reference to this article should be made as follows: Martin, J.K., Matela, R.J. and Sherwen, R.G. (2002) 'Modelling heat transfer through a novel design of rotary Kiln', *Int. J. of Computer Applications in Technology*, Vol. X, No. X, pp. 000–000.

1 NOTATION

A	area of cross section of heat flow
A_A	area of cross section of processing aggregate
c	specific heat capacity
h	heat transfer (film) coefficient
k	thermal conductivity
$k_{\rho l}$	thermal conductivity, lower density
$k_{\rho h}$	thermal conductivity, higher density
q	heat flow, radiation
Q	heat flow, conduction, convection
t	temperature
t_a	temperature, external ambient
t_w	temperature, external wall
x	direction of heat flow
ϵ	emissivity
ρ	density
σ	Stefan–Boltzmann constant

2 INTRODUCTION

The rotary kiln has been used since the late nineteenth Century. Conventional designs comprise essentially a circular cross section steel tube mounted on riding rings and rotated slowly about a longitudinal axis inclined a few degrees from horizontal. The inside of the tube is lined with a heavy refractory material such as fire bricks. A burner positioned at the lower end establishes a temperature gradient inside along the axis. Material to be processed feeds in at the cooler upper end and slowly makes its way under the influence of gravity towards the lower end, rising in temperature. The bed of process material within the tube is mixed as the tube rotates.

The object of the rotary kiln was to overcome the problem of uneven burning in the thermally more efficient shaft kiln. Despite higher fuel costs, the design

has become a workhorse of the processing industry and is in widespread use in various applications. It does however have many drawbacks such as high mass and rotary inertia, high capital and energy costs, thermal inefficiency, high thermal inertia exacerbating problems in lining maintenance, *etc*.

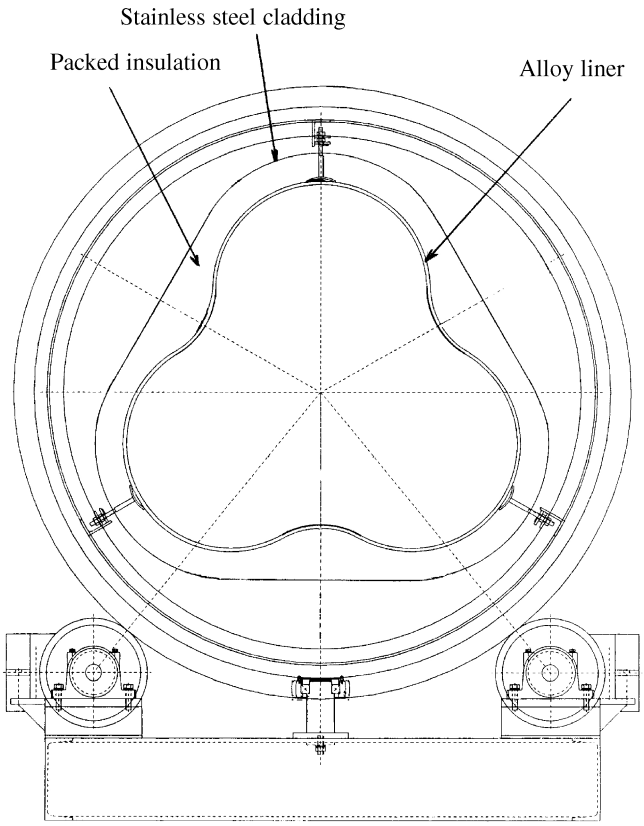

Figure 1 *Cross section of rotary kiln assembly.*

In the 1970s and early 1980s, Sherwen Engineering pioneered a new design of rotary kiln which contained a number of novel features made possible by recent advances in engineering materials [1, 2]. In brief, these were the use of a nickel chrome iron alloy to form a thin inner hot lining, a cross sectional trefoil shape for this inner lining and a surrounding insulation layer of alumina fibre. This trefoil kiln assembly provides an efficient alternative to the hot zone section of a conventional rotary kiln system used in processing plant, when operated in conjunction with vertical preheater kilns and driers, particularly for exothermic processing materials.

Figure 1 shows a cross section of the rotary kiln assembly with some details omitted for clarity. The inner lining is 3 mm thick and is surrounded by the thicker insulation layer consisting of densely packed alumina fibre matting, and the combination is held within a thin outer stainless steel cladding. In the longitudinal direction, the inner lining is formed with corrugations in the style of bellows, or a concertina effect, with pitch or 'wavelength' 50.4 mm and amplitude 5.5 mm. This is to accommodate longitudinal expansion and provide a key for gripping the insulation.

Figure 1 also shows an end riding ring and two support rollers. Figure 2 shows an overall view of the whole kiln assembly. The approximate outer diameter of the whole assembly is 1.8 m and the length just under 6.0 m. The frequency of rotation is 1.0 rev./min. The quantity of material being processed fills one of the three lobes of the trefoil cross section, as depicted in Figure 3, so on average the material is tumbled every 20 s giving a

Figure 2 *Trefoil rotary kiln hot section.*

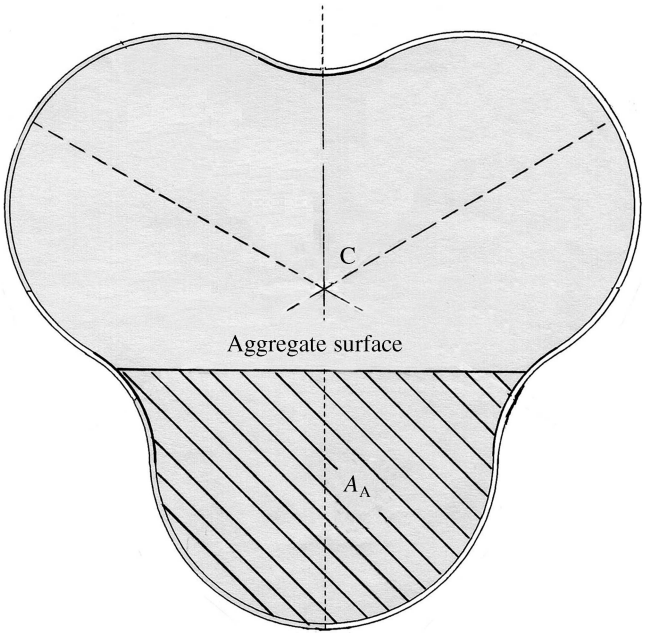

Figure 3 *Trefoil cross section with aggregate.*

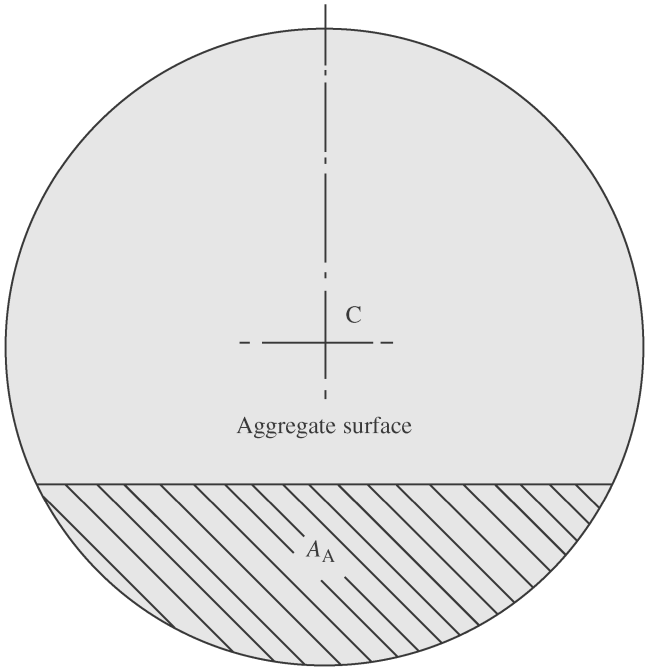

Figure 4 *Cylinder cross section with aggregate.*

frequent renewal of the exposed surface. The nature of the tumbling motion is steady and continuous giving a uniform renewal of the exposed surface and more consistent burning of the aggregate than in an equivalent circular section rotary kiln, shown in Figure 4.

The waste material to be processed was a combination of sewage sludge and pulverised fly ash, mixed with a clay binder, pelletised and dried. The background economics and processing characteristics of such materials have been reported by Sherwen [2]. One of the main characteristics of benefit is that such materials have an inherent calorific value. The material was to be processed at high temperatures to first burn out the carbon content at a minimum of 750°C, then at a minimum of 1150°C sintering into a lightweight inert aggregate. It was necessary therefore to maintain the bed of material at temperatures approaching 1200°C, aided by both the materials' own calorific value and the burner introducing hot gases of around 1600°C in the free space above the aggregate. These were the conditions for which the material selection was made and for which heat transfer through the composite section was modelled.

Early development was based on empirical results and data observed from tests with smaller scale kilns and experimental test fixtures. Lately, in view of the widespread availability of computer power and sophisticated finite element modelling systems, particularly for non-linear problems, the company embarked on a staged programme of analysis in parallel with the design and manufacture of the latest version of the kiln, to check various design parameters. This paper outlines the first stage of the approach used in the analysis and the significance of some of the results.

3 THEORETICAL MODELS

The process modelled was heat transfer in the forms of conduction, convection and radiation with the kiln not rotating. The plant's designers were primarily interested in the temperature of the free surface of the bed of process aggregate material when exposed to the hot conditions, and to the temperatures achieved at the kiln inner liner and exterior surfaces during steady-state operation. The effect of rotation was to steadily renew the free surface of the aggregate to expose fresh material to the given hot conditions. Heat was considered to flow from the hot interior through the composite cross section of inner liner, insulation and cladding, and then by convection from the external surface to the ambient air. Radiation from the external surface was not considered, an assumption based on the fact that external temperatures were targeted to be below 100°C. Within the kiln interior, heat was assumed also to be radiated directly from the inner liner interior wall to the aggregate surface, to and from the liner inner surface itself, and reflected in a diffuse manner from the liner surfaces to the aggregate surface. The effects of conduction between the liner and the surface of the aggregate was also considered, but not the effect of conduction into the bulk of the material. Also neglected were forced convection, direct radiation and conduction from the hot gases and any dust or ash particles within

the free space. The basic heat flow models were thus:

$$\text{Conduction}: \quad Q = -kA\frac{dt}{dx}$$

$$\text{Convection}: \quad Q = -h(t_a - t_w)$$

$$\text{Radiation}: \quad q = \varepsilon\sigma t^4$$

Computation models were 2D. The materials making up the composite conduction heat transfer path were assumed to be generally isotropic and tightly packed together with no local density variations or interface gaps. Thermal conductivity was generally allowed to vary with temperature for both the inner liner and insulation materials. For comparison purposes, some computations were made using constant averaged values for the insulation. Externally, convection from the outer surface was assumed to be mainly free but with a small degree of forcing possible due to atmospheric perturbations and the slow rotation. This was simulated by selecting a heat transfer coefficient value towards the upper limit of the range for free convection [3, 4]. Internally, it was assumed that a degree of roughness and oxidation would be present on the liner inner surface due to its operating environment, making it more akin to a grey body surface with an emissivity remaining constant with temperature [5]. The surface of the aggregate was also considered grey with constant emissivity.

Figure 3 shows the basic set-up of the trefoil model positioned with one of the three lobes at the lowest position. The nominal working surface level of aggregate is shown for the given cross sectional area A_A. Point C is the centroid of the trefoil cross section. Figure 4 shows the equivalent circular cross section model used for some comparative investigations, with point C again showing the centroid. The basis for equivalence was that the same cross sectional area of aggregate, A_A, was contained and the ratio of free space area to aggregate area was also the same for both kiln sections.

4 MATERIALS PROPERTIES

4.1 Working Aggregate

The dried and pressed input aggregate was in the form of granular pellets each 5–8 mm diameter. For the purposes of modelling, the working aggregate within the kiln was assumed to be amorphous and similar to clay, based on experience in handling the material. Quoted data for various forms of clay and other non-metallic materials were noted [3–6] and material properties assumed as below:

$c = 880.0\,\text{J/kg K}$
$k = 1.3\,\text{W/m K}$
$\rho = 1000.0\text{–}1460.0\,\text{kg/m}^3$
$\varepsilon = 0.45$

4.2 Inner Liner

The material used for the inner liner was an alloy of mainly nickel, iron and chromium designed for high temperature operations. Material data for such conditions are available from Accreditation Service certified laboratories [7] and independent suppliers and organizations such as the Nickel Development Institute. The main data derived from these sources are given in Table 1. Density was set as constant at $7940.0\,\text{kg/m}^3$. An average constant value of 0.8 was chosen for emissivity. Published values for thermal conductivity stopped at 1000°C and these were used even though a boundary condition inner surface temperature of 1200°C was specified. For one run, an extrapolated value for 1200°C was substituted for comparison purposes. For two runs, the thermal conductivity was reduced by 10% and 20% respectively to simulate changes of interior surface finish.

4.3 Insulation

The insulation was an alumina fibre produced in various forms for applications up to 1600°C. Its effective thermal conductivity depends on how it is laid and packed, and also on temperature. The type considered for this project was linear laid mat available in blanket form and of two different densities, 35 and $96\,\text{kg/m}^3$. Published data revealed that within the range of 200–1200°C, thermal conductivity increases by about 300% [8]. Also, at lower temperatures, the higher density material thermal conductivity was about 20% less than that for the lower density material, this difference decreasing steadily with temperature to about 6% at the higher temperatures [9, 10]. The material was in reality clearly not isotropic but tests had shown that if it was quite solidly packed then isotropy was a reasonably valid modelling assumption. The main data derived are given in Table 2. Specific heat capacity was quoted as $1.0\,\text{kJ/kg K}$ at 1000°C for both densities. For the simple comparative model data were assumed constant at the values for 600°C.

4.4 Outer Cladding

The outer cladding was to ASTM 304, a widely used stainless chromium nickel austenitic steel with good

Table 1 *Data for inner liner—Incoloy 800 HT.*

t (°C)	k (W/m K)	c (J/kg K)
200	14.8	498.9
400	17.9	545.1
600	21.1	606.8
800	24.7	660.1
1000	31.9	715.0

resistance to atmospheric corrosion. Grade 316 would be recommended if there is any likelihood of exposure to chloride solutions. Although 304 can be welded, the cladding was mounted by removable methods, so no effects due to hot working or treatment were considered. It was also assumed that the operating temperature of the outer cladding would be in the range 0–100°C so properties were taken as means for this range. A number of standard sources of data were consulted and the main data used are listed below. Computations were made with sheet thicknesses of 1.0, 2.0 and 3.0 mm.

$c = 500.0\,\mathrm{J/kg\,K}$
$k = 15.2\,\mathrm{W/m\,K}$
$\rho = 7905.0\,\mathrm{kg/m^3}$

Table 2 *Data for alumina fibre insulation—Saffil.*

t (°C)	$k_{\rho l}$ (W/m K)	$k_{\rho h}$ (W/m K)
100	—	0.045
200	0.062	0.05
400	0.081	0.065
600	0.106	0.086
800	0.139	0.117
1000	0.182	0.162
1200	0.239	0.224

5 COMPUTER MODELLING

5.1 Simplified Materials Section Model

Finite element models were developed using the Ansys modelling and finite element analysis package on an RM XP Twin PIII Xeon 550 MHz computer system. The first simplified model represented a small sectional piece of the composite materials assembly, both with and without the corrugation feature, and was used to check the effects of materials properties and dimensions on conducted and convected heat transfer. Figure 5 depicts the corrugated version. Both versions were of 1 m length (representing the circumferential direction straightened out) and 25.4 mm width (representing the longitudinal direction). The depth represented the radial thickness direction embracing the dimensions of the composite materials assembly at the narrowest region of the cross section, i.e. at the tip of a liner lobe. The featured corrugation was assumed to be of cosine wave form, and by symmetry a half-wave shape was sufficient for analysis. The models were each of planar form comprising 1360—8 noded quadrilateral elements.

5.2 Extended Cross Section Model

Figure 6 shows a further model for conducted and convected heat flow. This was based on a cross section

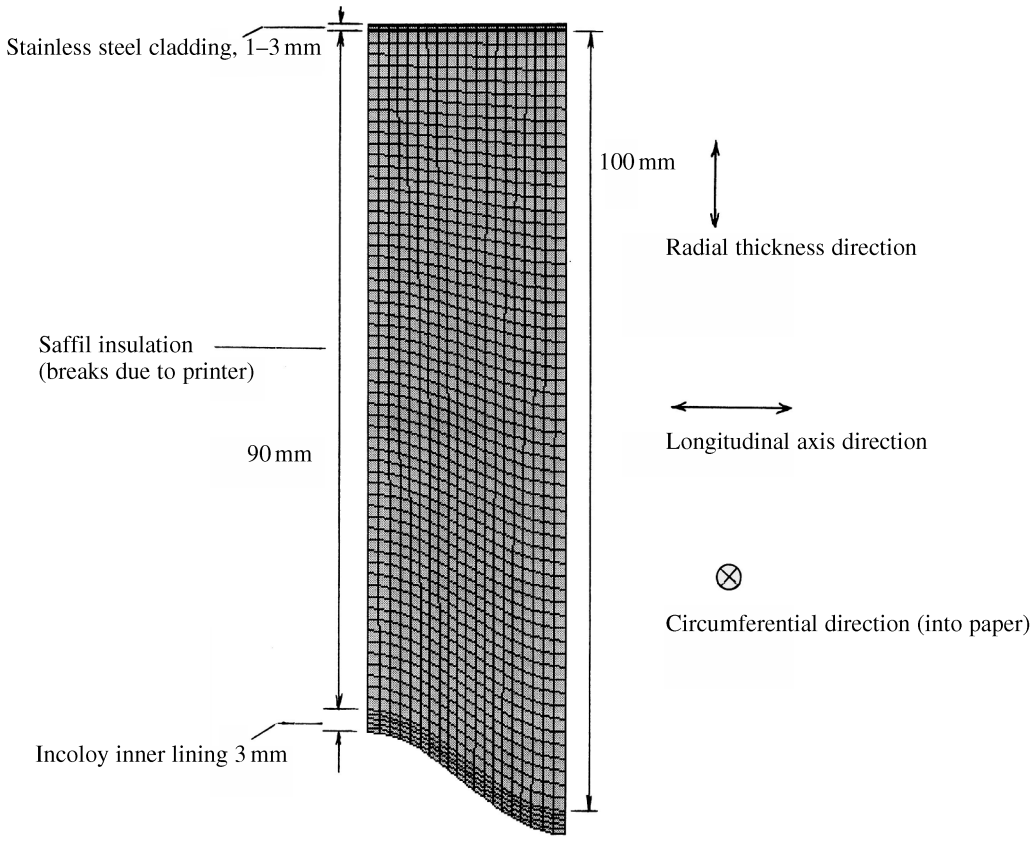

Figure 5 *Simplified materials section model.*

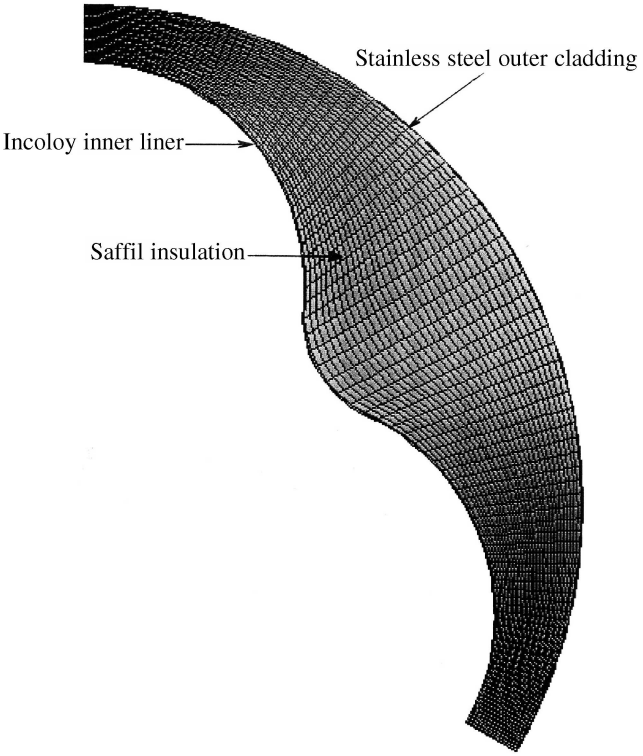

Figure 6 *Extended cross section model.*

of the kiln assembly split on planes of symmetry at the tips of two lobes of the trefoil, thus representing one-third of the complete cross section. The length of the model was 1.0 m, now corresponding in direction to the longitudinal axis of the kiln. Use of symmetry was possible for heat transfer analyses which neglected radiation, and a one-sixth cross section would have sufficed. The outer cladding was assumed to be of circular cross section giving a variable thickness of insulation. (This differed from the final practical design which incorporated flat surfaces between lobe extremities, as shown in Figure 1.) The stainless steel outer cladding was set at 2.0 mm thickness, and the inner liner 3.0 mm. The model was again of planar form comprising 3400—8 noded quadrilateral elements.

5.3 Radiation Models

As radiating surfaces may not support symmetry conditions, it was not possible to take advantage of any geometrical symmetry in the kiln cross section and so the radiating surfaces were modelled in full cross section. These radiating surfaces comprised the inner surface of the inner liner and the exposed surface of the contained aggregate. Two models were considered; one for the trefoil section, and one for the equivalent cylinder section, shown in Figures 3 and 4. The radiating surfaces were abstracted and modelled as two lines connected to form a closed system. One line, straight, described the exposed surface of the aggregate, the other, curved, described the inner surface of the liner. Upon these lines were superimposed a series of connected 2D conduction bar elements orientated to form a closed linked loop.

Each element had a radial depth of 3.0 mm (corresponding to the cross section radial direction) and notional length (in the kiln longitudinal direction) of 1.0 m. This gave a circumferential heat transfer conduction path of area 3000.00 mm^2. Each element had the ability to conduct heat between its two end nodes and supported a single degree of freedom, temperature, at each node. Each element also had associated with it relevant material properties, i.e. thermal conductivity, k, specific heat capacity, c, and density, ρ.

A hidden-line algorithm determined which elements were visible in terms of direct radiation to every other element. Radiation form factors were then calculated by first (a) enclosing each radiating or viewing element with a unit semicircle and (b) for each element all radiation target or receiving elements were projected onto its semicircle. In calculating a form factor, a predetermined number of simulated radiation rays, e.g. the default number of 200, were projected from a given viewing element onto its semicircle. The form factor was defined and evaluated as the number of rays incident on the projected semicircle surface compared to the number of rays emitted by the viewing element. These data for each element were held in matrix form written out to a holding file representing a super-element. The super-elements were then mapped onto the original conducting bar elements and appropriate boundary conditions set. The system, which was highly non-linear, was then solved to predict transient temperature rises in the aggregate surface.

5.4 Loads and Boundary Conditions

For the conduction and convection studies load cases were of two separate types. The first assumed fixed temperatures of a given value (usually 1200°C) applied to all nodes representing the interior surface of the inner liner. The second was an assumed heat flux applied to the inner surface of the liner and varied until the temperature of the inner surface reached about 1200°C for the given model and operating conditions. By this means, a comparative heat flux could be established for maintaining the given temperature profile. Most analysis runs simulated steady-state equilibrium conditions with some transient conditions representing the kiln warming up phases.

For the radiation studies, the conditions were generally fixed temperatures of 1100°C for the liner inner surface and 800°C for the initial temperature of the exposed surface of the aggregate. This represented pre-heated aggregate entering the kiln. By definition once thermal equilibrium had been reached there would be no net transfer of radiant heat to and from a given aggregate surface level (but in reality this surface is

constantly being renewed as the kiln rotates). Radiation analysis runs were therefore for short-term transient conditions for the stationary fixed level of aggregate representing the initiation of processing, for both the trefoil and cylinder section kilns.

An additional load case for the radiation studies for both cross sections was a simulated central heat source represented by a 250 mm diameter cylinder positioned about the centroid 'C' with its longitudinal axis coincident with the kiln longitudinal axis. The outer surface of this cylinder was maintained with a boundary condition temperature of 1500°C. This was to give some representation of the heat source when the gas burner was firing.

6 SIMULATIONS STUDIED

A large number of computations were carried out, both in validating models and considering various operating and analysis cases. A spreadsheet was made up to form a working map of computed scenarios and results. In general results comprised predicted temperature distributions throughout the composite materials assembly or plots of transient temperature rises for points of particular interest. Tables 3 and 4 summarize the main run parameters. For the studies in conduction and convection the main simulations covered the following:

1 Effect on temperatures of the corrugation feature in the design of the inner liner.
2 Effect on temperatures of varying the thickness of the stainless steel cladding.
3 Variation with temperature of thermal conductivity of the inner liner and insulation materials, and use of constant values.
4 Effect on temperatures of changes in the thermal conductivity of the inner liner to allow for surface oxidation and scale deposits.
5 Incorporation of insulation of reduced density.
6 Determination of heat fluxes required to maintain given temperature boundary condition values.
7 Comparison of transient temperature time histories incorporating changes in specific heat capacity of the inner liner material.
8 Comparison of temperature profiles achieved with simplified and extended model materials composite assemblies.

For the interior radiation studies, the main simulations covered the following:

1 For given initial conditions to compare the predicted aggregate surface temperatures after 20 s for the trefoil and cylinder cross sections, with and without the centralized heat source.
2 To isolate and consider the effect of conduction only from the liner into the exposed surface of the aggregate.
3 To isolate and consider the effect of radiation only to the surface of the aggregate.
4 To consider the effect of variations in the aggregate surface initial temperature and liner inner surface temperature.

Table 3 *Simple model run data.*

Run Index	*Corrugation Feature*	*Interior Boundary Conditions*		*Analysis Type*
		Heat	*Temperature (°C)*	
1	No	Fixed	1200	Steady state
2	No	Fixed	1200	Steady state
3	No	Fixed	1200	Steady state
4	Yes	Fixed	1200	Steady state
5	Yes	Fixed	1200	Steady state
6	Yes	Fixed	1200	Steady state
7	Yes	Flux	931	Steady state
8	No	Fixed	1200	Steady state
9	No	Flux	1195	Steady state
10	No	Flux	1195	Transient
11	Yes	Fixed	1200	Steady state
12	Yes	Fixed	1200	Steady state
13	Yes	Flux	1083	Steady state
14	Yes	Flux	1272	Steady state
15	Yes	Flux	1083	Transient
16	Yes	Flux	1083	Transient
17	No	Fixed	1200	Steady state
18	No	Flux	1255	Steady state
19	Yes	Fixed	1200	Steady state
20	Yes	Flux	1137	Steady state
21	No	Fixed	1200	Steady state
22	No	Fixed	1200	Steady state
23	Yes	Fixed	1200	Steady state

Table 4 *Simple model material specifications.*

Run Index	Inner Liner		Insulation			Outer Cladding	
	Thickness (mm)	k (W/m K)	Thickness (mm)	k (W/m K)	ρ(kg/m)^3	Thickness (mm)	k (W/m K)
1	3.0	31.9	95	0.086	96	1	15.2
2	3.0	31.9	95	0.086	96	2	15.2
3	3.0	31.9	95	0.086	96	3	15.2
4	3.0	31.9	90–100	0.086	96	1	15.2
5	3.0	31.9	90–100	0.086	96	2	15.2
6	3.0	31.9	90–100	0.086	96	3	15.2
7	3.0	31.9	90–100	0.086	96	2	15.2
8	3.0	31.9	95	Variable	96	2	15.2
9	3.0	31.9	95	Variable	96	2	15.2
10	3.0	31.9	95	Variable	96	2	15.2
11	3.0	31.9	90–100	Variable	96	2	15.2
12	3.0	40.3	90–100	Variable	96	2	15.2
13	3.0	31.9	90–100	Variable	96	2	15.2
14	3.0	31.9	90–100	Variable	35	2	15.2
15	3.0	31.9	90–100	Variable	96	2	15.2
16	3.0	31.9	90–100	Variable	96	2	15.2
17	3.0	31.9	95	0.106	35	1	15.2
18	3.0	31.9	95	0.106	35	1	15.2
19	3.0	31.9	90–100	0.106	35	1	15.2
20	3.0	31.9	90–100	0.106	35	1	15.2
21	3.0	28.7	95	0.086	96	2	15.2
22	3.0	25.5	95	0.086	96	2	15.2
23	3.0	Variable	90–100	Variable	96	2	15.2

7 PRACTICAL MEASUREMENTS

It is hoped that practical design aspects and tests will be published subsequently. Brief experiments have however been carried out on the protoype trefoil kiln depicted in Figure 2 and micro-structural analyses made of one that has been subject to service conditions. For the prototype version, temperatures were measured by TCL K-type sprung thermocouples positioned on the outside surface of the inner lining at the lobe position. A Eurisem ST 504 hand held roving thermocouple was used to measure surface temperatures of the stainless steel outer casing. A Minolta/Land Cyclops 52 hand held pyrometer was also used to estimate inner lining interior surface temperatures. Emissivity levels were set either at 0.9 or 1.0, a variation which had little effect on displayed results.

The kiln was operated as normal in open air but in an empty condition with vented insulated capping panels fitted at each end. Heat was supplied by the burner at a rate somewhat less than the stoichometric rating of 250 kW, such that the liner temperature reached 1150°C from winter time ambient in 1.5 h. At this time, the outer casing surface temperature was 80°C as recorded at random positions. The burner heat input was then reduced by about 90% which was sufficient to maintain inner temperatures, and this heat soak phase was maintained for a further 3 h. Thermal equilibrium had been established and the external surface temperature was recorded as 100°C.

For the service kiln material samples were taken from three different regions of the inner liner. These were metallurgically polished and etched using standard preparation techniques and the microstructure inspected with an optical microscope. A range of samples was also prepared using material that had not been subject to any service temperatures and artificially aged in a high temperature furnace to provide baseline comparisons of microstructures known to have been subject to temperatures from 900°C to 1500°C. Comparisons of grain boundaries and known alloy depositions suggested that the service temperatures may have approached 1300°C, i.e. in excess of the required optimum of 1200°C.

8 SUMMARY OF RESULTS

Predicted outer surface temperatures using the first simplified models were consistently of the order 5–6% higher than those for the extended second model, for similar loads and boundary conditions. The simplified first model could therefore be used with a degree of confidence to compare, e.g. the effects of changes in material parameters. Example plots are shown in Figure 7 for the simplified model (non corrugated), and in Figure 8 for the extended model.

A significant result, depicted in Figure 9, is that for all conditions studied the predicted outer surface temperature was well below 100°C, and in most cases below 80°C. These findings are in accordance with results observed from a smaller model [1], and would represent a significant saving in energy over conventional designs where temperatures of over 200°C are common, for similar operating conditions and kiln interior

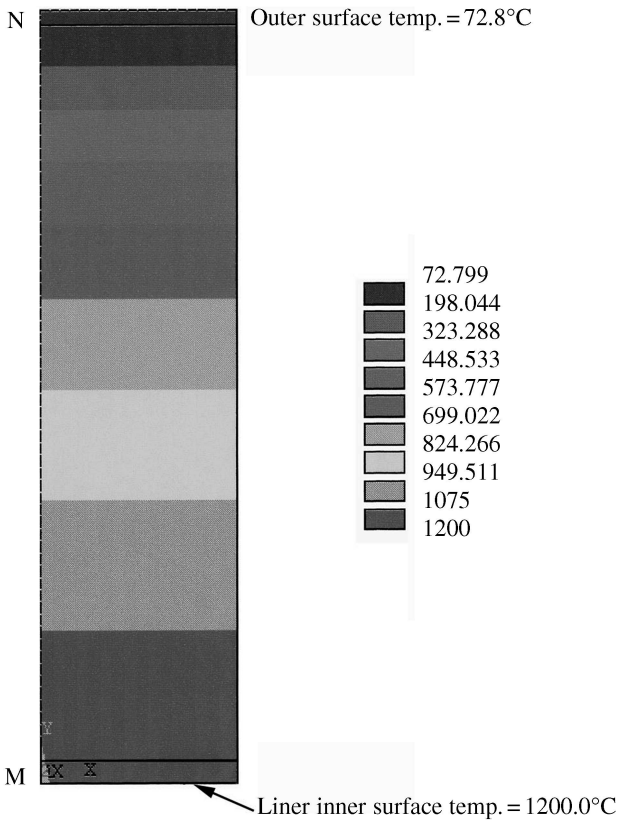

Figure 7 *Simplified model temperature plot.*

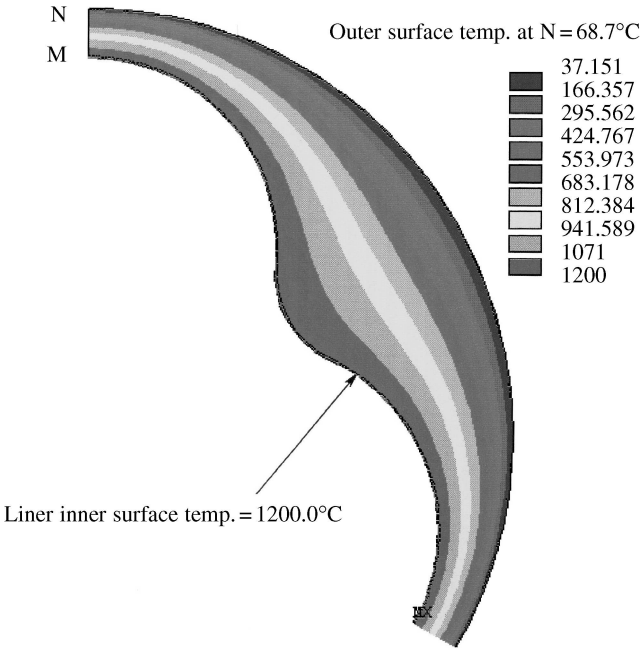

Figure 8 *Extended model temperature plot.*

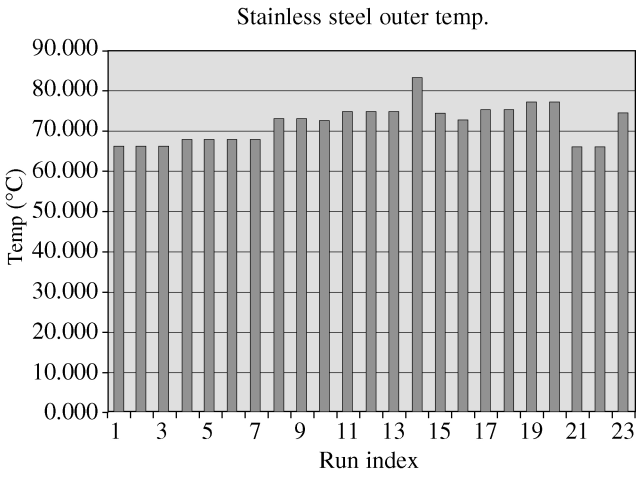

Figure 9 *Predicted outer surface temperatures.*

temperatures [1]. The test measurements for a kiln operating without contained aggregate showed external temperatures of 80–100°C, slightly in excess of those predicted but still significantly less than for conventional designs. In practice, additional insulation could be used to reduce the outer surface temperature still further with very little weight penalty, but with mainly exothermic processes an outer surface temperature of 100°C represents a reasonable balance between capital and process costs.

Variation of the thickness of the stainless steel outer cladding between 1 and 3 mm had a negligible effect on heat transfer and temperature profiles. The effect of the corrugation feature in the inner liner was to consistently increase outer surface temperatures by between 2% and 3%. Significant changes in values of thermal conductivity for the inner liner had little effect on predicted temperature profiles, as did allowing it to vary with temperature. It was also shown that for both steady-state and transient conditions after 60 s there was a negligible temperature gradient through the 3 mm thickness of the inner liner.

The significant variation with temperature of thermal conductivity of the insulation had a relatively small effect when compared to using the nominal fixed value for 600°C. With fixed uniform inner surface temperatures, and for the higher density insulation, incorporating a temperature dependent variable thermal conductivity insulation increased predicted outer surface temperatures by 3.1% for the maximum and 4.5% for the minimum. For the lower density insulation, the increases were 7.5% and 3.5% respectively. Thus, the effect was more pronounced with the lower density insulation in the hottest region. Using a constant mid range value for k could still therefore be a useful exercise, e.g. in approximate manual calculations.

With fixed uniform inner surface temperatures and for the variable conductivity insulation the effect of reduced density was to increase the maximum outer surface temperature by 11.1% and the minimum by 5.9%. For the same inner boundary conditions, the minimum outer surface temperatures occurred adjacent to the thickest portion of insulation, and were of the order 40–50% of the maximum temperatures. This predicted

circumferential temperature gradient endorsed the design decision to reduce the insulation thickness in the coolest regions as shown in Figure 1.

With a uniform working heat flux applied to the interior surface and starting from ambient conditions the predicted time taken for the inner surfaces to reach 1000°C was between 5 and 8 h, influenced by the values chosen for specific heat of the inner liner. Transient predicted temperatures were asymptotic in form with time and represented a warm up rate of about one-third that quoted for conventional designs [1]. In practice, the warm up time could be reduced even more to about 1 h by application of extra burner gas.

In terms of internal radiation, with the cylinder section, for a fixed uniform inner surface temperature of 800°C and a central heat source at 1500°C; after 20 s the temperature of the aggregate surface had increased to 968°C near the wall, and to 1131°C at the centre. The temperature distribution across the surface was near linear. The figures for the same points and conditions for the trefoil section were 968°C and 1260°C respectively rising greater than linear across the surface. Figure 10 shows these results.

The effect of increasing the fixed uniform inner surface temperature to 1100°C was to raise the lowest temperatures of the aggregate surface by about 25% for both sections. With radiation isolated, the effect of conduction from the liner to the surface of the aggregate was to increase temperatures by less than 2.0% after 60 s, in both kiln cross sections. This highlighted the importance of the direct radiation from the interior hot surface of the inner liner when it was hotter than the aggregate.

For all runs in which radiation was invoked as the primary means of heat transfer an average of over 98% of the aggregate target temperature of 1100°C was achieved after 60 s, with 1000°C being achieved after 20 s. This suited the frequency of rotation and surface renewal in the real situation.

Practical results have indicated that the computer model predicts both interior and exterior temperatures quite close to those required for optimum processing and that warm up rates are also comparable. Development of the computer model could include further work on the simulation of the degree of forced convection from the external surfaces, conduction within the main body of the aggregate itself, and possibly longer term the dynamic modelling of the tumbling and mixing action within using a discrete element approach. Operation of the practical kiln system has highlighted a need for a precise control of interior temperatures to avoid the possibility of overheating the inner liner.

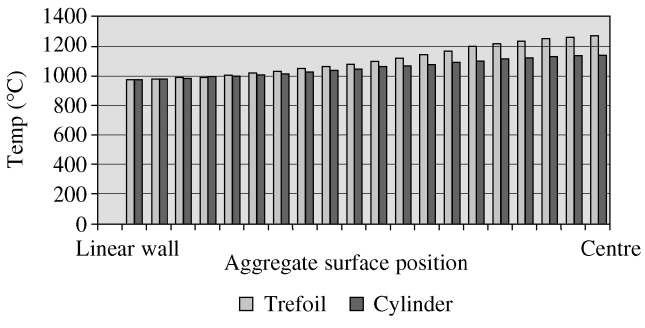

Figure 10 *Aggregate predicted surface temperatures after 20 s.*

9 CONCLUSIONS

A number of computer models have been set up to model the heat transfer characteristics of a novel rotary kiln design. These have consistently predicted external surface temperatures significantly reduced in comparison with conventional designs of rotary kiln.

It was beneficial in both understanding and verification to adopt an approach starting with simple small sectional models, building up to more comprehensive models. It was noted, e.g. that using an averaged constant value for the thermal conductivity of the insulation produced results that were well within 10% of those allowing for its variation.

The models have illustrated the contributions to overall performance of materials data and properties such as thicknesses of sections, non-linear variations in thermal conductivity, changes in specific heat capacity, surface finishes and emissivity.

It has been shown that in terms of modelled interior radiation, the trefoil section gives higher aggregate surface temperatures than the cylindrical section for the same cross sectional areas, capacity and materials of construction.

The models have indicated that, in terms of heat transfer and insulation performance, the novel kiln design is fundamentally sound requiring no changes to the construction and operating conditions, and have highlighted one or two areas where minor changes may be made to economic advantage.

The practical tests (without contained aggregate) indicated a warm up rate significantly faster still than those of conventional designs, and of the theoretical model, in terms of inner surface temperatures. Tests also showed that for steady-state conditions the theoretical model produced results quite close to values observed so far. Observations from a service kiln have shown that interior processing temperatures have been maintained in use.

ACKNOWLEDGEMENTS

The authors gratefully acknowledge the support of Sherwen Engineering Co. Ltd, and The Open University.

REFERENCES

1 Parks, L.F. and Sherwen, R.G. (1986) 'The use of new materials in an improved design of rotary kiln', *Materials and Design*, Vol. 7, No. 5, pp. 252–255.
2 Sherwen, R.G. (1994) 'The process of making synthetic aggregates from mixtures of waste materials', Joint Inst. Civil Eng. and Malaysia Inst. Eng. Conference on *solid and industrial waste management systems*, Kuala Lumpur.
3 Incropera, F.P. and De Witt, D.P. (1990) *Fundamentals of heat and mass transfer*, John Wiley & Sons.
4 Rogers, G.F.C. and Mayhew, Y.R. (1980) *Engineering thermodynamics, work and heat transfer*, Longman.
5 Gray, W.A. and Muller, R. (1974) *Engineering calculations in radiative heat transfer*, Pergamon Press.
6 Sparrow, E.M. and Cess, R.D. (1978) *Radiation heat transfer*, Hemisphere Publishing Corp.
7 Inco Alloys International (1997) *Incoloy Alloys 800, 800 H and 800 HT*, Inco Alloys International Inc.
8 ICI (1999) *Saffil alumina fibre—product data sheet*, ICI Saffil Business.
9 Horn, F.L., Filo, J.A. and Powell, J.R. (1981) *Thermal conductivity measurements of insulators for fusion Blankets, J. of Nuclear Materials*, pp. 103–104.
10 Saffil Ltd. (1999) *Saffil blanket—product data sheet*, Saffil Ltd.

BIOGRAPHY

J.K. Martin, Lecturer in Mechanical Engineering, Open University, since 1982. Founder head of Open University Lubrication Research Group. Visiting Lecturer in Computer Aided Engineering, Cranfield University, UK. Actively involved in producing Finite Element Analysis educational material for 10 years. Former posts include 5 years (1977–1982) as Senior Engineer and Project Manager at Aston Martin Lagonda Ltd, Newport Pagnell, UK, engaged in the design and development of quality performance cars. Four years (1973–1977) in Vehicle Engineering Directorate at Ministry of Transport, London, UK, working on national and international legislation and standards for motorcycle, car and pedestrian safety. Graduated from Cranfield with M.Sc. in 1974, and Ph.D. in 1997, specializing in fluid film lubrication.

R.J. Matela, Lecturer in Design Engineering, Open University, since 1976, with a two year period in the Biology Department researching Mathematical/Theoretical Biology problems of cellular self sorting and molecular protein conformation. Involved with Finite Element Analysis for 15 years and as an Engineering Consultant for 10 years. Currently, sub-dean (facilities) within the Faculty of Technology. Since 1994, have been actively involved in producing Finite Element Analysis educational material for professional engineers and postgraduate students. Have been an active member (Finite Element Analysis) of the Solder Research Group, The Open University, Material Engineering Department, since 1998. Graduated from University of Waterloo, Canada, with Ph.D. in Systems Design in 1976.

R.G. Sherwen, Joined Blyvooruitzicht Gold Mining Company, South Africa, in 1953 and took Government exams to become a Certificated Engineer Mines and Works. In 1956 joined the G.E.C. UK Atomic Energy design team. In 1957 was appointed project manager for G.E.C of the Hunterston A Nuclear Power Station, seeing the project through to operational, legal and financial completion. In 1970 joined Sherwen Engineering and has specialized in the design of novel plant and equipment for high temperature thermal processing. Graduated from London University, UK, with a B.Sc. in Mechanical Engineering in 1951.